# Terahertz quantum cascade lasers

Alessandro Tredicucci
Lukas Mahler
Tonia Losco
Jihua Xu
Cosimo Mauro
Rüdeger Köhler
Fabio Beltram

Laser action at THz frequencies has recently been demonstrated in quantum cascade (QC) structures, thanks to the use of superlattice active material and to the implementation of a waveguide concept based on surface plasmon propagation. Since then, improved fabrication has led to continuous-wave operation and high output powers. Thanks to the introduction of new design concepts, lasers operating at ever longer wavelengths and higher temperatures are being realized and the first practical applications are being developed.

Here we present recent advances in technologically relevant aspects like single-mode devices and tuneability. In particular distributed optical structures are analysed, as well as the potential of external cavity set-ups. We also discuss issues in laser design related to the emission frequency, and demonstrate the excellent control achievable through quantum engineering and MBE growth.

Stable single-mode emission at a precisely designed frequency is highly desirable for most applications. For this purpose, the concept of distributed feedback (DFB) can be successfully implemented also in THz QC devices [1-8].

The peculiar surface-plasmon structure of the waveguide requires the realization of rather unconventional DFB gratings for the diffraction of light propagating along the laser ridge. In the first devices a periodic corrugation has been etched into the thin highly-doped semiconductor contact layer underneath the top metallization. This causes a modulation of the real part of the modal refractive index; lasers featuring such grating still display a regularly spaced Fabry-Perot spectrum, but with two modes strongly suppressed, as can be seen by the red curves in Fig. 1. This is a typical feature of index-coupled DFB lasers with only moderate coupling strength but strong reflectivity at the Fabry-Perot facets.

In order to enhance the coupling constant and increase mode discrimination, an additional loss modulation was introduced by depositing and annealing GeAu/Au contacts selectively on the crests of the etched grating. Thus, complex-coupled DFB resonators, which are much more effective in achieving single-mode operation than bare index-coupled devices, are obtained with an estimated coupling constant of 4 $cm^{-1}$. Figure 1 shows the spectra (blue lines) of two such devices (length 3.2 mm and $L = 9.2\,\mu m$ in one device and 4.4 mm with $L = 9.4\,\mu m$ in the other).

Lasing takes place within the previously observed stop-band, as expected for a complex-coupled DFB laser. The coupling is now sufficient to achieve single mode operation under all injection currents and operating temperatures.

The technique just described produces gratings with rather limited coupling coefficients, thereby making long laser cavities necessary for the achievement of single-mode operation. This affects device performance, increasing driving currents and hindering lasing in continuous wave mode. The issue becomes more and more relevant going towards longer emission wavelength as the DFB grating period has to be proportionally enlarged.

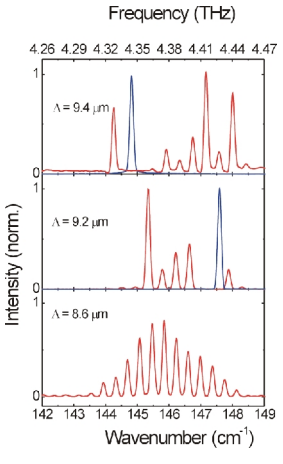


Fig. 1
Spectra of five different DFB lasers with grating periods of 9.4, 9.2 and 8.6 $\mu m$, respectively, collected at an injection current close to the maximum output power. Red lines correspond to spectra recorded from devices in which the distributed feedback was implemented only by removing 150 nm of the top contact layer. Blue lines are spectra recorded from devices in which an additional loss-modulation was introduced by an annealed-contact grating.

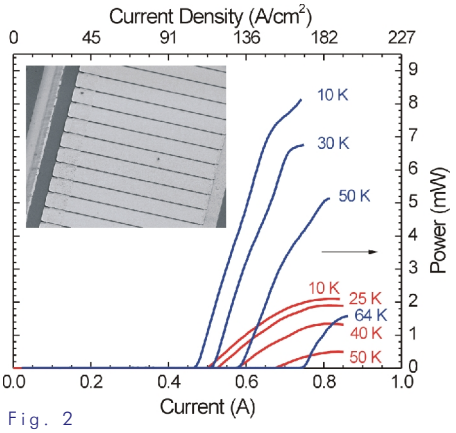


Fig. 2

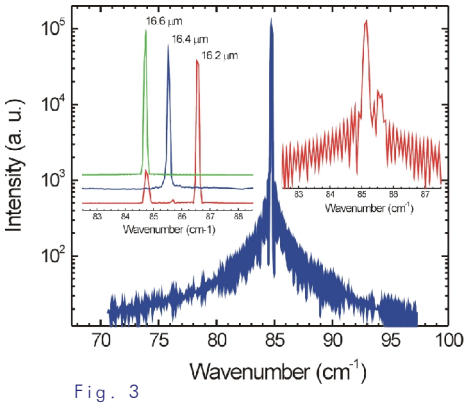


Fig. 3

Fig. 2
Light-current characteristics of a 2.5 THz DFB QC laser. Blue lines refer to pulsed operation with 5% duty-cycle and were collected from one facet with f/1 parabolic optics on a calibrated pyro-elelectric detector; red lines were obtained mounting a Winston cone in front of the laser and using a pyro-electric power meter (33% estimated collection e.ciency). The inset shows a scanning-electron microscope picture of a surface-plasmon DFB grating.

Fig. 3
Single-mode emission spectrum in logarithmic scale of a 2.5 THz DFB laser with a 16.5 $\mu$m slit periodicity and narrow top metallization. It was collected in pulsed mode at 1% duty-cycle and 0.92 A drive current, close to the maximum output power. In the left inset we plot the spectra of three lasers with different DFB periods and wide metallization. The upper two were collected close to threshold, while the lowest one at a higher current in order to well show the DFB mode here somewhat detuned from the maximum gain (hence the presence also of Fabry-Perot modes). The right inset shows a spectrum at higher current of the 16.4 $\mu$m laser of the left inset. The appearance of a second transverse mode is clearly evident.

An elegant way of realizing a one-dimensional photonic crystal for surface plasmon modes has been recently demonstrated [9]. A slit opened in the metallic layer acts as a barrier for the wave propagation as no surface plasmon is supported there. Part of the light is reflected back, part transmitted by tunneling across the slit, and part is scattered out of the interface mode.

A periodic series of slits acts then as a photonic crystal structure, and, if the slits are sufficiently thin (much narrower than the wavelength), this can be accomplished with minimal scattering losses.

We have applied this idea to the fabrication of DFB quantum cascade lasers emitting near 2.5 THz (a relevant frequency for ozone detection). The procedure follows the one of Ref. 10 until the deposition of the last metallic layer. This is in fact patterned by electron-beam lithography with a series of slits at the L/2 DFB period (see inset of Fig. 2). E-beam lithography, while not necessary for resolution reasons, is very useful in this first experiment to easily vary the grating period and test different slit widths. For the latter, the best compromise between grating strength and diffraction losses is found at approximately 2 $\mu$m width (close to 10% of the period length). Single-mode operation is obtained in pulsed and continuous-wave, with a side-mode suppression ratio of at least 20 dB, as can be seen in the spectrum of Fig. 3. The position of the emission peak shifts with the grating period, in reasonable agreement with the computed modal refractive index of 3.65.

It is interesting to notice that, contrary to the one depicted in Fig. 2, the first devices featured a top-metallization extending to the very edge of the ridge, in order to leave a larger area for bonding. However, they frequently showed operation on more than one transverse mode, as exemplified in the right inset of Fig. 3; a narrower metallization has then been adopted to solve this issue. The procedure can be further simplified avoiding the lift-off step. In this case the resist used in the lithographical process fills the slits, with the final gold layer covering everything. While the operating principle is analogous, this possibility simplifies bonding and in general yields better performance, probably owing to decreased scattering losses. The output power of one such DFB laser, approximately 2 mm long, is plotted as a function of drive current in Fig. 2. The emission is single mode in the whole current and temperature ranges, with about 8 mW measured at 10 K and a low threshold current density of about 100 A/cm2.

The successful development of THz QC lasers towards widespread use in real-world applications has also to go through the establishment of various technical details, which become of relevance when the production of commercial systems and devices is considered. The versatility of frequency design is now clear, with the whole range from 2.1 THz to 4.8 THz well coverable. An important aspect, however, is the reliability, precision, and repeatability of the relation between predicted and actual emission wavelength.

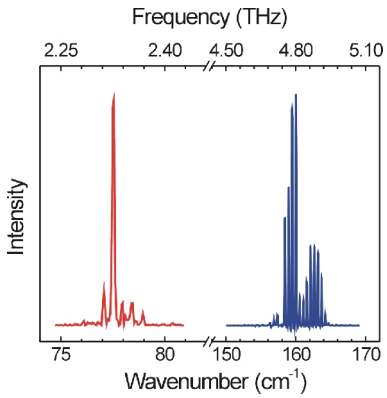


Fig. 4
Fabry-Perot emission spectra of quantum cascade lasers operating near 2.3 THz and 4.8 THz.

As an example we show in the Fig. 4 the spectra of two lasers realized for the desired frequencies of 4.76 THz (important for monitoring atomic oxygen) and 2.31 THz. Obviously the experimental results are very much on target with the expectations, but there are a few further characteristics that have to be pointed out. Both lasers are based on the same BTC concept for the active material and on the conventional waveguide design, which testifies their broad applicability. In reality the 2.3 THz laser waveguide features two buried highly-doped layers, instead of the usual one, under the active core. This solution allows the possibility of controlling separately the boundary conditions of the surface plasmons on the two sides, thereby resulting in a better compromise between optical losses and confinement factor. In the case of the 2.5 THz sample a confinement factor of about 48 % is reached, with 10 $cm^{-1}$ absorption losses. These values easily permit the use of such waveguides even at long wavelengths, providing very low threshold currents and high output powers, as can be seen in Fig. 5. It is also worth remarking that the design of the active region of the 2.3 THz sample was derived from the 2.5 THz one by just increasing the thickness of two barriers of 1 Å each and that of a well of 3 Å the injection barrier had to be reduced by 3 Å to fit the modified active region). The precise shift of emission frequency, corresponding to about 1 meV, and the very similar performances attest the high reliability and control of modeling and growth, and of their mutual relationship, even at this rather extreme level.

The ability to tune the emission wavelength of single-mode devices is fundamental for spectroscopic applications. THz DFB lasers can be tuned by temperature or drive current much in the same way as conventional DFB laser diodes. The limited range of operating temperatures and the low emission frequency results, however, in a small tunability of only a fraction of cm-1.

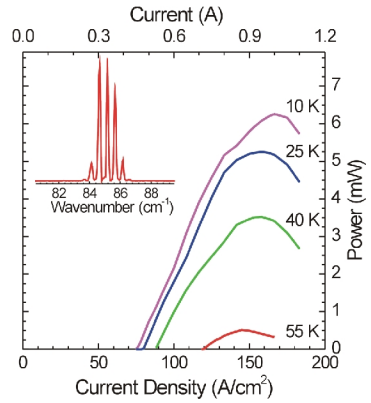


Fig. 5
Continuous wave light-current characteristics (33 % estimated collection efficiency) of a 3.2 mm long quantum cascade laser operating near 2.5 THz. In the inset a typical emission spectrum is displayed.

This number could still be reasonable in some applications, but poses a too precise requirement on the fabrication side to be feasible in a relatively high-yield manufacturing effort. It is therefore crucial to implement cavity solutions allowing for broad tunability on ranges comparable to the gain width. The simplest idea would be to use an external cavity set-up with a rotating diffraction grating as is often done with visible and near-IR diode lasers.

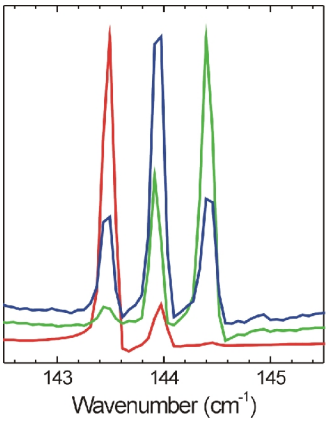


Fig. 6
Emission spectra from a 4.4 THz QC laser in an external Littröw cavity. The output has been collected from the laser back-facet, opposite to the one facing the grating. The three curves have been obtained varying the angle between grating and laser, and are normalized for clarity.

Here complications arise from the absence of good refractive optics, the large divergence of the output beam, and most of all from the di.cult implementation of anti-reflection coatings, necessary to suppress Fabry-Perot oscillation on the internal cavity modes and to reduce reflection losses.

In Fig. 6 we show preliminary spectra from a 4.4 THz QC laser within an external cavity in the Littröw configuration. In this case the facet facing the diffraction grating was angled at 5°, still away from the Brewster angle but enough to reduce the strength of Fabry-Perot modes. Light was collected with a f/0.75 off-axis paraboloid and sent on a grating with 20 grooves/mm and a blaze wavelenght of 46.67 mm. The spectra clearly still show the internal Fabry-Perot structure, but the intensity can be shifted from mode to mode by rotating the external grating, and the power output is enhanced in the best situation by an order of magnitude with respect to the no-grating configuration.

References

[1] R. Köhler, A. Tredicucci, F. Beltram, H. E. Beere, E. H. Linfield, A. G. Davies, D. A. Ritchie, R. Iotti, and F. Rossi, "Terahertz semiconductor-heterostructure laser, " Nature 417, 156-159 (2002).
[2] M. Rochat, G. Scalari, D. Hofstetter, M. Beck, J. Faist, H. Beere, G. Davies, E. Lin.eld, and D. Ritchie, "Continuous-wave operation of far-infrared quantum cascade lasers," Electron. Lett. 38, 16751676 (2002).
[3] S. Barbieri, J. Alton, S. S. Dhillon, H. E. Beere, M. Evans, E. H. Linfield, A. G. Davies, D. A. Ritchie, R. Köhler, A. Tredicucci, and F. Beltram, "Continuous-wave operation of terahertz quantum-cascade lasers," IEEE J. Quantum Electron. 39, 586591 (2003).
[4] R. Köhler, A. Tredicucci, F. Beltram, H. E. Beere, E. H. Linfield, A. G. Davies, D. A. Ritchie, S. Dhillon, and C. Sirtori, "High-performance continuous-wave operation of superlattice terahertz quantum-cascade lasers," Appl. Phys. Lett. 82, 15181520 (2003).
[5] S. Kumar, B. S. Williams, S. Kohen, Q. Hu and J. L. Reno, "Continuous-wave operation of terahertz quantum-cascade lasers above liquid-nitrogen temperature," Appl. Phys. Lett. 84, 2494-2496 (2004).
[6] R. Köhler, A. Tredicucci, C. Mauro, F. Beltram, H. E. Beere, E. H. Linfield, D. A. Ritchie, and A. G. Davies, "Terahertz quantum-cascade lasers based on an interlaced photon-phonon cascade," *Appl. Phys. Lett.* 84, 12661268 (2004).
[7] L. Ajili, G. Scalari, J. Faist, H. E. Beere, E. H. Linfield, D. A. Ritchie, and A. G. Davies, "High power quantum cascade lasers operating at l ~ 87 and 130 μm," *Appl. Phys. Lett.* 85, 39863988 (2004).
[8] L. Mahler, R. Köhler, A. Tredicucci, F. Beltram, H. E. Beere, E. H. Linfield, D. A. Ritchie, and A. G. Davies, "Single-mode operation of terahertz quantum cascade lasers with distributed feedback resonators,"*Appl. Phys. Lett.* 84, 54465448 (2004).
[9] J. C. Weeber, Y. Lacroute, A. Dereux, E. Devaux, T. Ebbesen, C. Girard, M. U. Gonzalez, and A. L. Baudrion, "Near-field characterization of Bragg mirrors engraved in surface plasmon waveguides," *Phys. Rev. B* 70, 235406 1-12 (2004).
[10] R. Köhler, A. Tredicucci, F. Beltram, H. E. Beere, E. H. Linfield, A. G. Davies, D. A. Ritchie, S. Dhillon, C. Sirtori, Appl. Phys. Lett. 82, 1518 (2003).